Iraqi Journal of Agricultural Sciences –2026:57(2):663-675
P-ISSN: 0075- 0530 /E-ISSN: 2410-0862
DOI: https://doi.org/10.36103/x6kpsf31

METAL COMPLEXES OF CURCUMIN AND DMB LIGAND , GEOMETRICAL AND BIOLOGICAL

Fatima R. A. , Hasann A. H.
Dept. Chem. Coll. Educ for Pure Sci (Ibn Al- Haitham), University of Baghda,

ABSTRACT

This study was aimed to investigate synthesis and characterization of two ligands type (azo-linked Schiff-base) with its complexes. Precursor (W) obtained by reaction of diazonium salt of 1-Naphthyl amine with O-tolidin in water as a solvent *via* 2:1 mole ratio. Azo-linked Schiff-base ligands synthesized *via* the reaction of 3, 3'- dimethyl-5,5'-bis((E)-pyridin-3-yldiazenyl)-[1,1'-biphenyl]-4,4'-diamine with curcumun or dibenziyl methan for obtaining 4, 4', 4'', 4'''- ((1E, 1'E, 6E, 6'E) - ((3, 3'- dimethyl-5, 5'-bis((E)-pyridin-3-yldiazenyl)-[1,1'-biphenyl]-4,4'-diyl) bis (azaneylylidene)) bis (5-hydroxyhepta-1,6-diene-1,7-diyl-3-ylidene))tetrakis(2-methoxyphenol) (H_2L^1) or 3,3'-((3,3'-dimethyl-5,5'-bis((E)-naphthalen-1-yldiazenyl)-[1,1'-biphenyl]-4,4'-diyl)bis(azaneylylidene))bis(1,3-diphenylpropan-1-ol) (H_2L^2). Complexes synthesis achieved via reaction of the metal ion salts CoII, MnII, CuII, NiII and CdII with azo-linked Schiff-base ligands within (2-1) mole ratio. Characterization of prepared ligands and complexes through spectroscopic and analytical techniques included; conductance, microanalysis, thermal analysis and magnetic susceptibility (for complexes) measurements along with NMR, UV-Vis and FTIR spectroscopies

Keywords: azo , curcumin , di bnzaiylmethan, schiff base, , tolidin, ,1-naphthyl amine
*** Part of Ph.D. dissertation of 1st author**

Received: 23/9/2023, Accepted: 17/1/2024, Published: 28/2/2026

INTRODUCTION

The functional group (-N=N-) characterizes azo compounds (Reham &Hassan , 2022), which may use as dyes and the most synthetic important colorant agent, widely applied in: paper manufacturing, printing and textile, etc. Azo compounds have the ability to have biological effectiveness (Rehab &Al-Hassani, 2016). Reaction of the azo compounds with schiff bases formed Azo-schiff base type compounds (Haider & Karam,2022). The academic and applied researcher focused on this type of compounds, which have been used in various fields in science, medicine and technology. Azo-schiff base compounds were used in manufacturing of dyes, which belong to coloration character intensity of these ligands, this may resulted from the delocalization of pi electrons, also the containment of the azo methane and azo moieties, enabling their uses in dyeing fabrics and polyester, acrylic and nylon threads (Bashandy *et al*,2016, El-Sonbati *et al*,2016). In our labs, it was reported many azo linked Schiff bases and their transition metal complexes,(Enaam *et al*,2020, Hasan *et al*,2013). The multiple functional groups presence in a molecule improves properties, therefore; in our research, we attempted to synthesize, characterize and bio-reactivity study of ligands type azo-Schiff base owing both imine and azo moieties along with hetero and homo aromatic rings, the ligands derived from curcumun (Zaid &Alrubeii, 2023) or dibenziyl methan with tolidine and 1-Naphthyl amine. Also transition metal complexes prepared and studied.

MATERIALS AND METHODS

FT-IR spectral data were determined using Fourier Transform Infrared Spectra apparatus

Iraqi Journal of Agricultural Sciences –2026:57(2):663-675
P-ISSN: 0075- 0530 /E-ISSN: 2410-0862
DOI: https://doi.org/10.36103/x6kpsf31

FTIR-600, as Potassium bromide discs, in 4000-400 cm^{-1} range. An internal reference, tetra methyl silane (TMS), in DMSO-d^6 solvent to assess some synthesized compounds ^1H and ^{13}C- NMR spectra using a Brucker 400 MHZ instrument (100 MHz for 13C and 400 MHz for 1H). The electronic (U.V-Vis) spectral data were obtained with a quartz cell of (1.0), at 25 °C, with Shimadzu UV-160 spectrophotometer using DMSO-d^6 as a solvent. Electrospray (+) mass spectrophotometer type a Sciex Esi mass analyzer to obtain mass spectra, Euro EA 3000 apparatus were used for the ligands' elemental analysis (C.H.N.) and Shimadzu (A.A) 680G atomic absorption spectrophotometer for metal content determinations. Stuart apparatus of type SMP40 electro-thermal was used to estimate melting points of prepared compound.

Synthesis of azo ligands

Figuer (1) shows precursor compound (W) were synthesized by dissolving 1-naphthyl amain (0.5g, 3.49 mmol) in water (10 ml) and 3 ml of hydrochloric acid, this mixture was agitated until a clear solution obtained, and it was then stored at a temperature of 0 to 5 °C. Then, a drop wise addition of a sodium nitrite aqueous solution (1g, 14.49mmol) in 5ml of water was made while maintaining a pH of about (Eman *et al*,2020) and a temperature below 5°C. Tolidine ((0.37g, 1.74 mmol) solutions, and an equivalent volume of NaOH was added to the diazonium salt solution, before being dried at pH 6-7, the precipitate was filtered and repeatedly rinsed with cold water. After that curcumin or dibenzayl methan solution was added (0.74g, 2.01mmol) or (0.43g,1.92mmol) respect to azo derivative (0.5g, 0.96mmol) W with a few drops of glacial acetic acid as a catalyst, refluxed 10 hrs., before the precipitate compound was obtained by filtration, the solution leaved at room temperature for about 15 minutes.(Said *et al*,2017) Table (1): displays the physical properties of the synthesised precursors and ligands

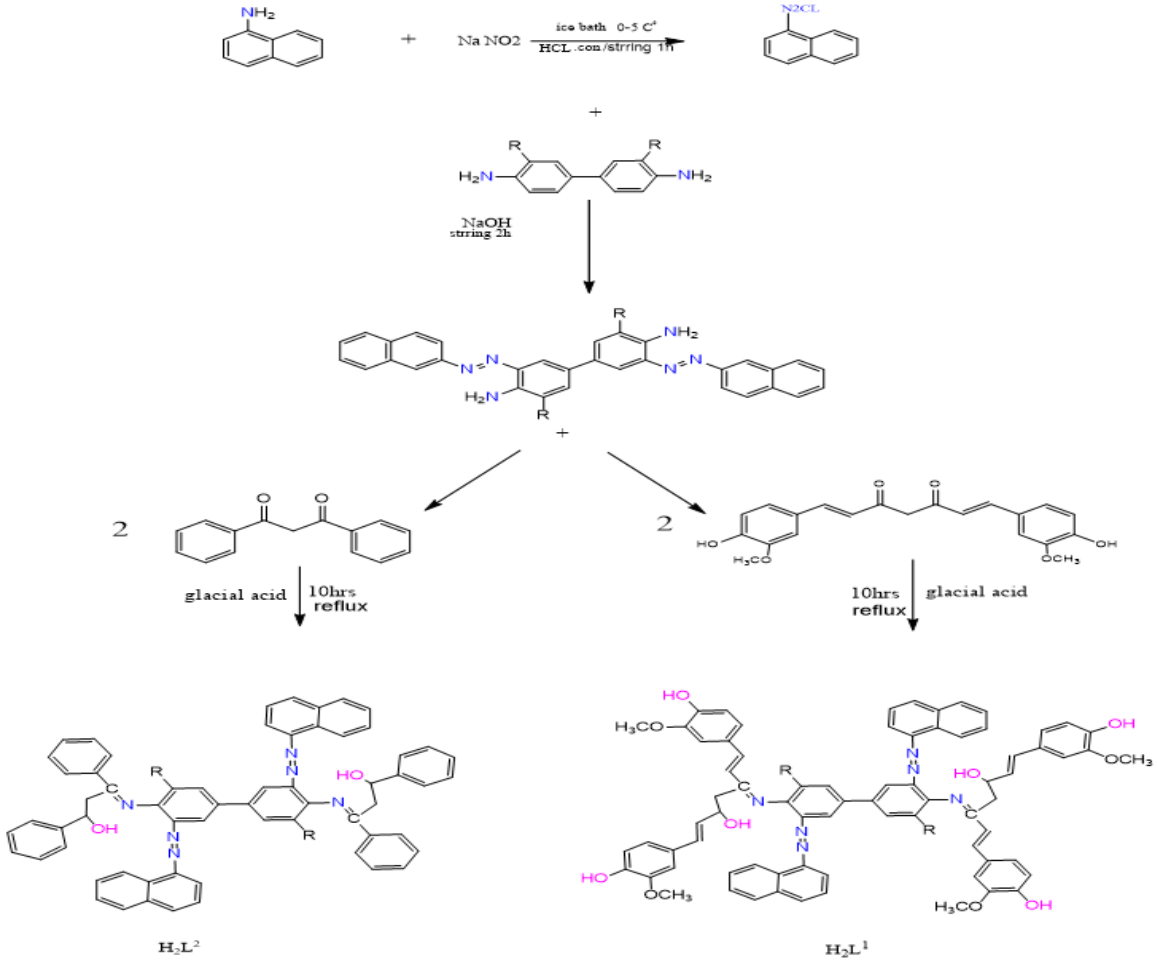

Figuer 1. Synthetic route for Precursors and ligands

Iraqi Journal of Agricultural Sciences –2026:57(2):663-675
P-ISSN: 0075- 0530 /E-ISSN: 2410-0862
DOI: https://doi.org/10.36103/x6kpsf31

Table 1. colours, melting points, Weight and yields of the precursor and ligand

m.p. °C	Color	Yield (%)	Weight of azo (g)	Weight of amine (g)	Precursor
0.5	Dark Purpl	165	85%	1.54	W
0.5	Violat	109	94%	1.11	H_2L^1
0.5	Violat	79	95%	0.85	H_2L^2

Synthesis of complexes

Figure (2) shows synthesis of complexes achieved through adding an ethanolic potassium hydroxide solution equivalent amount (10) ml with heating and stirring to a solution of (0.5 g, 0.40 mmol) or (0.5g, 0.53mmol) from the ligands [H_2L^1] or [H_2L^2] dissolved in (40 ml) of ethanol. Equivalent amount of each metal salt [CdII, MnII, CoII, NiII and Cu II dissolved in 10 ml ethanol was added to ligands solution. The resulting mixture was refluxed for 2 hrs., then washed with ethanol and recrystallized. Analysis of microelements and calculated values include: practically C (72%) H (5.5%) N (7.2%); theoretical C (73%) H (5.3%) N (7.9%); [H_2L^2]: practically C (71%) H (5.5%) N (9.9%) theoretical: C (72%) H (5.8%) N (9.7%). (Hasan &Fluorescence, 2017). Table (2)and (3): displays the physical properties of the synthesised complexes.

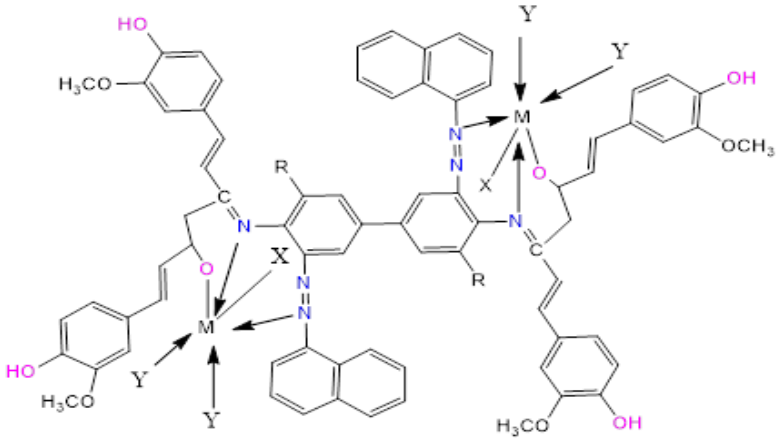

H_2L^1

Were M=Mn, Ni, Co , Y=H_2O X=Cl
Were M= Cu , Cd, X=Cl, Y=0

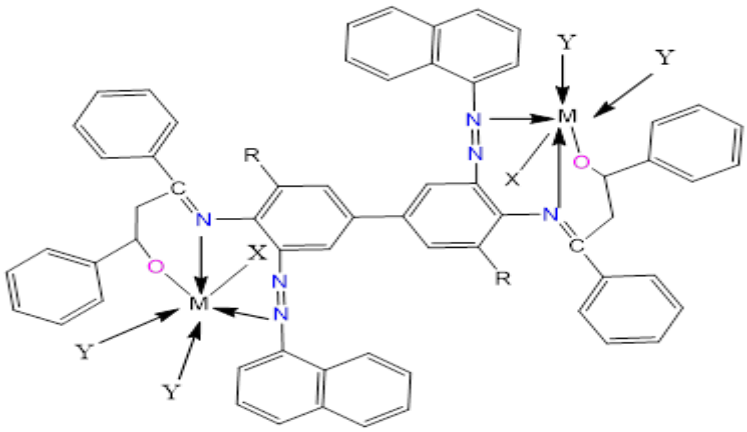

H_2L^2

Were M=Mn, Ni, Co ,X=Cl, Y=H_2O
Were M= Cu , Cd, X=Cl, Y=0

Figuer 2. Synthetic route of complexes

Iraqi Journal of Agricultural Sciences –2026:57(2):663-675
P-ISSN: 0075- 0530 /E-ISSN: 2410-0862
DOI: https://doi.org/10.36103/x6kpsf31

Table 2. Some physical properties for complexes of [H_2L^1]

Complex of Metal ions	Molecular Formula	M.Wt	Weight of metal salt(g)	The complex Weight(g)		color	m.p.C	Yield
$[Co_2(H_2L^1)(H_2O)_4Cl_2]$	$C_{76}H_{74}Co_2\ Cl_2N_6O_{14}$	1475.76	0.3	0.33		green	>300*	91
$[Ni_2(H_2L^1)\ (H_2O)_4Cl_2]$	$C_{76}H_{74}Ni2\ Cl_2N_6O_{14}$	1467.76	0.5	0.31		red	>300*	86
$[Cu_2(H_2L^1)\ Cl_2]$	$C_{68}H_{60}Cu_2\ Cl_2N_6O_{10}$	1417.76	0.2	0.20		Brown	>300*	86
$[Cd_2(H_2L^1)\ Cl_2]$	$C_{68}H_{60}Cd_2\ Cl_2N_6O_{10}$	1515.76	0.3	0.32		Yellow	>300*	86
$[Mn_2(H_2L^1)(H_2O)_4Cl_2$	$C_{76}H_{74}Mn_2\ Cl_2N_6O_{14}$	1473.76	0.3	0.32		red	>300*	88

Table 3. Some physical properties for complexes of [H_2L^2]

Complex of Metal ions	Molecular Formula	M.Wt	Weight of metal salt(g)	The complex Weight(g)		color	m.p.C	Yield
$[Mn_2(H_2L^2)(H_2O)_4Cl_2]$	$C_{64}H_{54}Mn_2\ Cl_2N_6O_6$	1188.75	0.5	0.32		red	159	88
$[Co_2(H_2L^2)(H_2O)_4Cl_2]$	$C_{64}H_{54}Co_2\ Cl_2N_6O_6$	1189.5	0.2	0.21		Green	175	84
$[Ni_2(H_2L^2)\ (H_2O)_4Cl_2]$	$C_{64}H_{54}Ni2\ Cl_2N_6O_6$	1182.5	0.5	0.57		Orange	197	90
$[Cu_2(H_2L^2)\ Cl_2]$	$C_{68}H_{60}Cu_2\ Cl_2N_6O_2$	1132.5	0.3	0.31		Green	194	86
$[Cd_2(H_2L^2)\ Cl_2]$	$C_{68}H_{60}Cd_2\ Cl_2N_6O_2$	1230.5	0.3	0.33		Yellow		

RESULTS AND DISCUSSION

The precursors produced using a conventional azo dye method. The 2:1 mole ratio reaction between 1-Naphthyl amine diazonium salt and O-Tolidine. Look at Scheme 1. precursors W reacted with curcumin or di bnzayl methan to produce [H_2L^1] and [H_2L^2], which were then used as the ligands of azo-linked Schiff bases. (Scheme 1 and Scheme 2). The complexes created by reacting the metal salts of Cd II, Mn II, Co II, Ni II, and Cu II in a 2:1 mole ratio with the azo-linked Schiff base ligands. Elemental analyses, electronic spectra, FT-IR data and magnetic susceptibility measurements, all supported the novel compounds' existence. The suggested structures supported by the analytical results in Table 4. The complexes' molar conductance in DMSO solvents is indicative of electrolyte and non-electrolyte behavior. As a result of complex formation, the ν(C=N) at ca. (1647, 1639) cm-^{1} in the free ligands were shifted and appeared at lower frequencies in the complexes spectra, recorded a reduced in bond order, and appeared at (1620-1624) cm-^{1} . Bands in the (1400–1454) cm-^{1} range were categorized as belonging to the (N=N) azo group. This shift in the two groups insured the involvement and coordination of the C=N and N=N moieties to the metallic center.(Baidaa *et al*,2021) . The delocalization of the metal electron density into the ligand -system, which reveals the participation of the azo and imine groups in the coordination, may be the cause of the shift in frequency in these bands.(HOMO-LUMO), where HOMO is the highest Lowest Unoccupied Molecular Orbital, or HOMO, is the highest occupied molecular orbital and.(Mustafa *et al*,2021) The complexes exhibited at lower frequencies bands around (401–497) and (501– 578) cm^{-1} which may referred to(M–O) and (M– N) stretching vibration respectively. The (M–O) band noticed at higher frequency ranges compared to (M–N), this could belong to the change in (dipole moment) value for M–O when compared to M–N. (Dhekra & Mahdi, 2023)

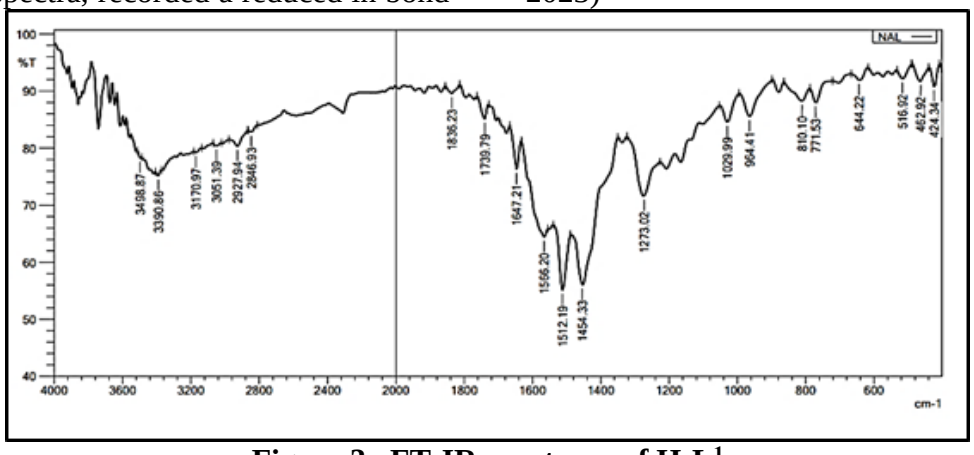

Figure 3. FT-IR spectrum of H_2L^1

Iraqi Journal of Agricultural Sciences –2026:57(2):663-675
P-ISSN: 0075- 0530 /E-ISSN: 2410-0862
DOI: https://doi.org/10.36103/x6kpsf31

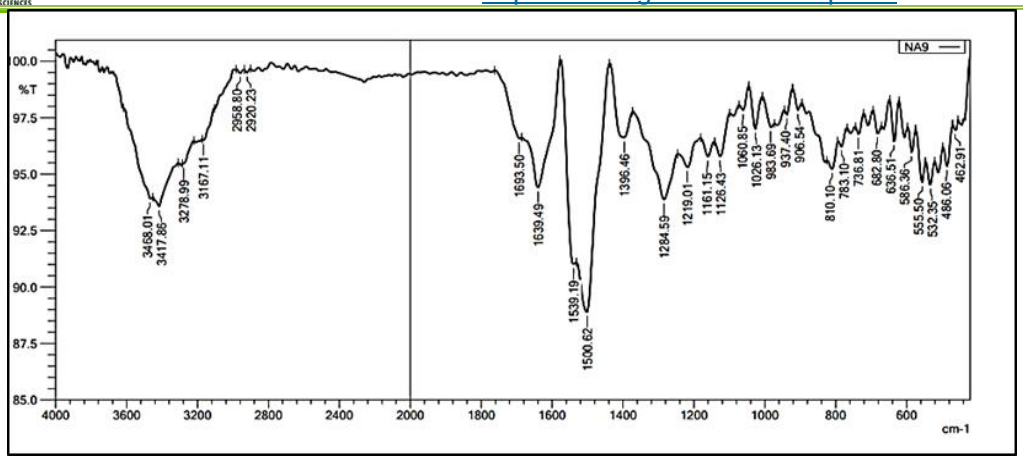

Figure 4. FT-IR spectrum of H_2L^2

Mass spectrometer

Mass spectra of the Schiff base ligand, [H_2L^1] spectrum in Figure (5) exhibits a distinct molecular ion peak at m/z = 1222.76amu, which coincides (M + 1) with the molecular composition of the Schiff base ligand ($C_{76}H_{68}N_6O_{10}$). The fragments are shown by a series of peaks in the [H_2L^1] ligand's spectrum at m/z 650, 574, 524, 433, 496, 212, 369, 195, 247, 144, and 128 amu. These peaks' intensity reveals the stability of the parts.in Figure (6) A peak in the mass spectrum of [H_2L^2] at m/z+=937 amu, attributable to [M+1] of the ligands' chemical formula ($C_{64}H_{52}N_6O_2$), Also observed at the same time peaks at 863, 786, 639, 485, 383, 225, 212, 156, 149, 160, 110, 136,88, 78, and 56 amu, which the fragments . (Ali *et al*,2007).

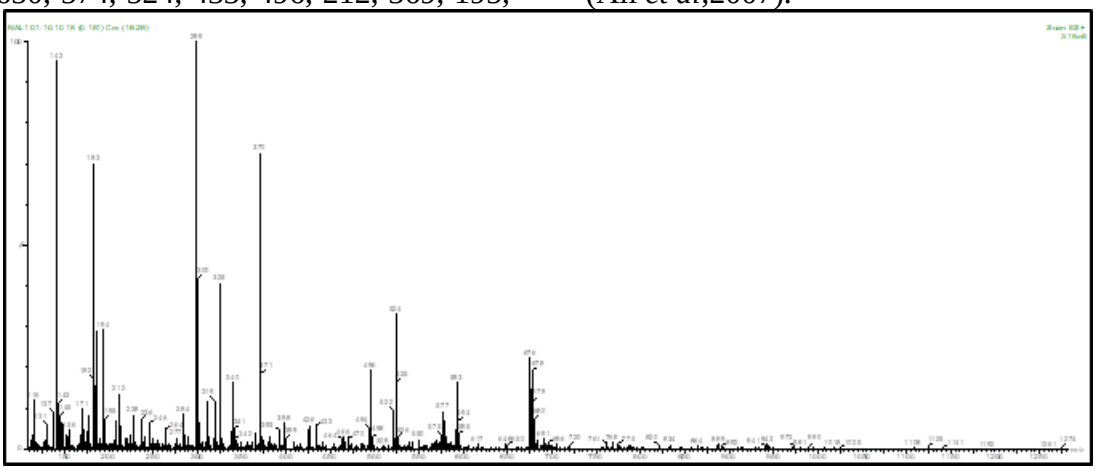

Figure 5. mas spectrum of

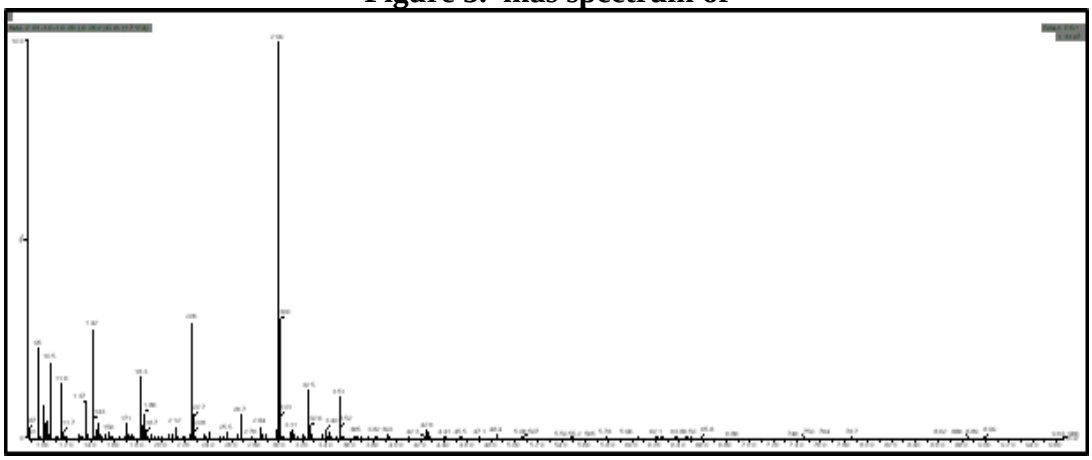

Figure 6. mas spectrum of H_2L^2

Electronic spectral data for the ligand and complexes: The chelation between metal ions and the azo linked Skiff base ligand causes the π-π* and n-π* transitions of the conjugated

Iraqi Journal of Agricultural Sciences –2026:57(2):663-675
P-ISSN: 0075- 0530 /E-ISSN: 2410-0862
DOI: https://doi.org/10.36103/x6kpsf31

chromophore to change in energy, which is connected to the blue shift behavior of complexes. It is possible to attribute the considerable hypochromic shift in the π-π* and n-π* transition regions caused by the dye's complexation with the metal ion to the complex's M-L charge transfer transition. An electronic transition in a conjugated system, in which a metal may or may not participate and may be assigned to M-L charge transfer transition for the complexes, is thought to be the cause of the light absorption in metal chelates, which is thought to occur in the UV area.(Mohammad *et al*,2010)

The absorption peaks for H_2L^1 and H_2L^2 are((213, 213), (212, 345) nm, respectively, relating to overlaps of π→π* and n→π* are caused and (422,424) Due to the transition of the N=N group(24). The Mn(II) complex $^6A_1g \rightarrow ^4T_1g(G)$, $^6A_1g \rightarrow ^4T_1g$ transition assigned by peak at (819), (717) nm indicates a deformed octahedral geometry around the Mn(II) ion for H_2L^1 and H_2L^2 respectively . Due to the C.T and $^4A_2g^{(F)} \rightarrow ^4T_1g^{(F)}$, $^4T_1g^{(F)} \rightarrow ^4T_2g^{(F)}$ transitions, the Co(II) complex exhibits additional peaks in the d-d region at 422, 618, and 776 nm, and 424, 745 nm in $[H_2L^1]$and $[H_2L^2]$respectively. The octahedral geometries around the Co atom in Co(II) complexes with this spectrum are deformed.(Shaima & Salih, 2022) A deformed octahedral geometry around the Ni atom was corroborated by peaks in the Ni(II) complex at 445and 777 nm and 359,709 nm that were attributed to C.T and $^3A_2g \rightarrow ^3T_1g^{(F)}$ transitions, for $[H_2L^1]$and $[H_2L^2]$ respectively(Muntaha &Majeed, 2023, Said et al,2020). The H_4L^1 and H_2L^2 Cu(II) complex spectrum has shown peaks in the regions (420 ,772) nm and (364,748) nm due to C.T and d-d transitions type $^2B_1g(^F) \rightarrow ^2B_2g(^F)$ respectively. The spectrum of the $[H_2L^1]$ and $[H_2L^2]$ CdII complex exhibited peaks at (267,345) and (268,421) assigned to ligand π–π * and M→ L charge transfer. (Naureen *et al*,2021)

^{1}H AND ^{13}C –NMR spectra of azo

The NMR spectra were recorded in DMSO-d^6 (dimethyl sulfoxide) using tetramethylsilane (TMS) as standard. Table 4 shows the spectral data of ^{1}HNMR of the azo compound W, as displayed in Figure (7) The resonance at (δ=8.00-9.00) ppm referred for four (NH_2) protons, the (C-H) aromatic protons showed signals at (δ=7.51-7.94) ppm, while the signals referring to the aliphatic CH_3,CH_2 appeared at (δ=1.98, 2.37) pm (7) The ^{13}C-NMR spectral data for (W) shown in Table (4) , the spectrum revealed aromatic carbon atoms are located at (δ=123.52-129.80) ppm, while the carbon of the imine(C=N) group signal appeared at (δ=185) ppm. The chemical shift at (δ=123.58-129.88) ppm may referring to the(C-N, C-O and C-C) In Figuer (8). The deference in signals results from the deference in the electronic environment surrounding the groups.

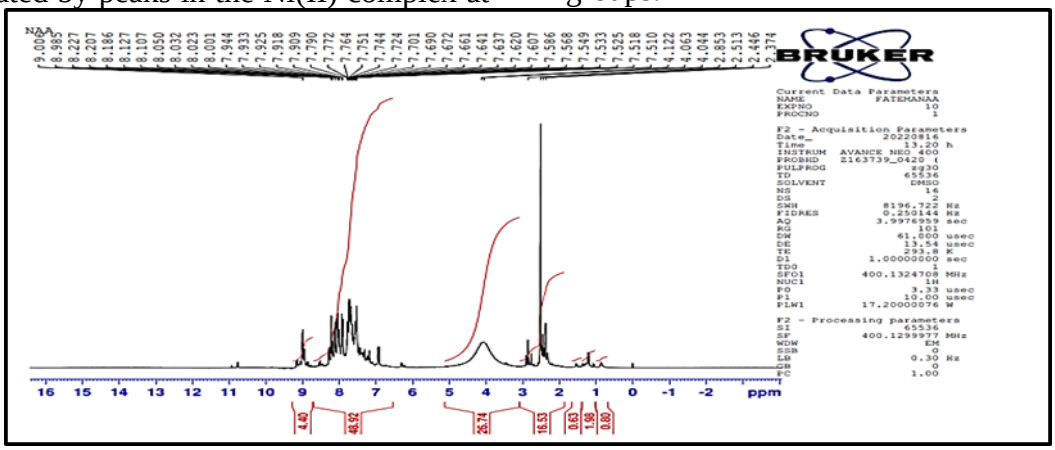

Figuere 7. Spectrum of ^{1}H-NMR for (W)

Iraqi Journal of Agricultural Sciences –2026:57(2):663-675
P-ISSN: 0075- 0530 /E-ISSN: 2410-0862
DOI: https://doi.org/10.36103/x6kpsf31

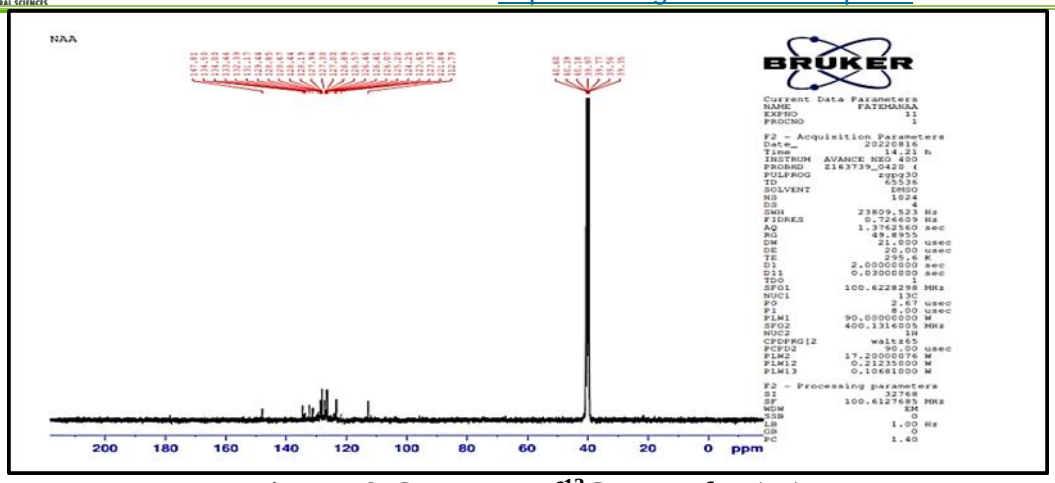

Figuere 8. Spectrum of ^{13}C-NMR for (W)

Table 4. ^{13}CNMR –H-NMR and spectral data of the W

Funct. Group	H-NMR (ppm)	13C NMR (ppm)
C=N	_____	185
-NH2	8.00-9.00	___
-CH3	1.98	2.37-2.85
-CH2	2.37-2.85	40.18-49.87
-CH arom	7.51-7.54	123.52-129.80
-C-N ,C-O and -C-C-	___	132.16-136.70
C=C		93.72
DMSO-d_6	4.04-4.12	

Schiff base ligands [H_2L^1] , [H_2L^2] ^{1}H-nmr and ^{13}C –nmr spectra

In Figuer (9) and (11), the OH groups (resulted from tautomerization of the curcumiin and dibenziyl methan moiety resonances shifted to the upper field and appeared at (6.05), and (6.89) for [H_2L^1] and [H_2L^2] respectively. This may attributed to the intramolecular hydrogen bonding (OH...N=C).(Muna &Kareem,2020) While (CH_3) protons were given the chemical shift between (1.21) and (1.07) ppm. The (-CH_2) was attributed to the strong peaks at (2.51) and (2.50) ppm. The aromatic protons of [H_2L^1] and [H_2L^2] may be attributed to the numerous chemical shifts around (7.17-8.98) and (7.36-8.97) ppm, respectively. The chemical shift caused by the DMSO-d6 protons was lastly seen in the spectra at (3.80-40.62) and (3.42- 4.89) ppm (Aemed &Enaam ,2022; Wasan *et al*,2019) .^{13}C-NMR in Figuer(10)and (12) the [H_2L^1] and [H_2L^2] regions with ppm values between (δ=111.81–130.80) and (δ=111.69–129.32) can be assigned to the C-O, C-N, and C-C groups in the two ligands respectively. Aromatic (C=C) for [H_2L^1] and [H_2L^2] is responsible for the chemical shift at the ranges of (δ=131.17-141.18) and (δ= 133.50-147.80) ppm.While the carbon atom (C=N) azomethine groups in the [H_2L^1] and [H_2L^2] are responsible for the chemical shifts at (δ=148.46) and (δ=185.80)ppm, respectively. signals at (δ=93.72)and (δ=93.72) refers to (C-OH)alif for [H_2L^1] and [H_2L^2], respectively. In the azo-linked Schiff base compounds, the carbonyl group C=O that was produced by the tautomerization of the dipnzeyl methan moiety was lastly observed at about (δ=183.68) and (δ=196.20)ppm for [H_2L^1] and [H_2L^2] respectively.(Kheirkhahi *et al*,2021)

Iraqi Journal of Agricultural Sciences –2026:57(2):663-675
P-ISSN: 0075- 0530 /E-ISSN: 2410-0862
DOI: https://doi.org/10.36103/x6kpsf31

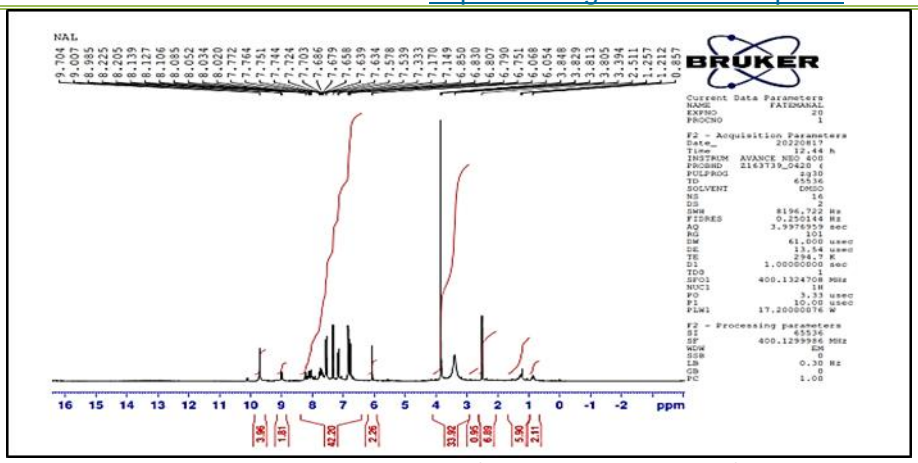

Figure 9. Spectrum of ^{1}H-NMR for (H_2L^1)

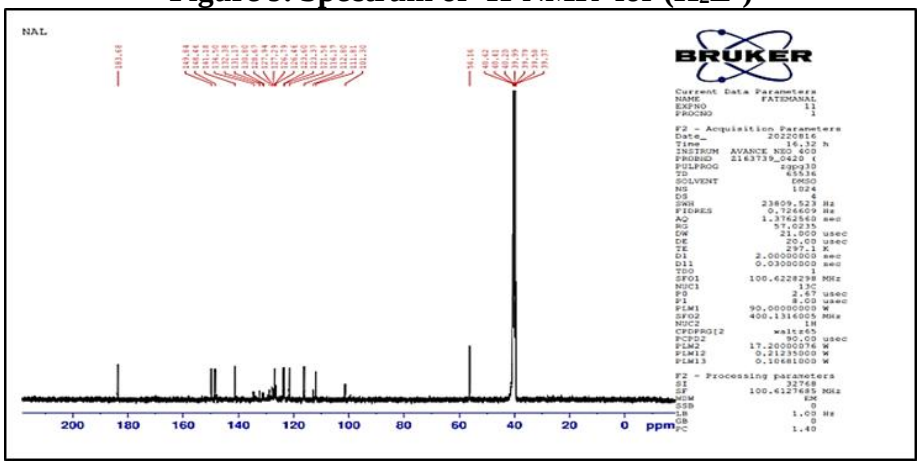

Figure 10. Spectrum of ^{13}C-NMR for (H_2L^1).

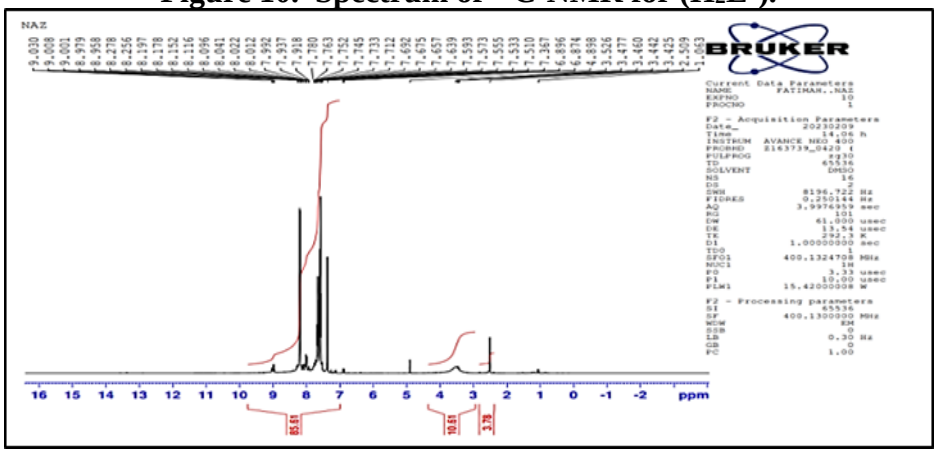

Figure 11. Spectrum of ^{13}C-NMR for (H_2L^2).

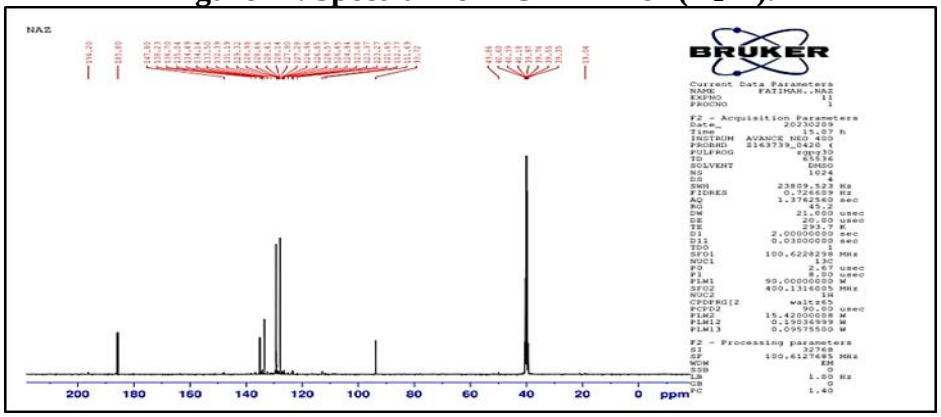

Figure 12. Spectrum of 1H-NMR for (H_2L^2).

Iraqi Journal of Agricultural Sciences –2026:57(2):663-675
P-ISSN: 0075- 0530 /E-ISSN: 2410-0862
DOI: https://doi.org/10.36103/x6kpsf31

Thermal analysis

Three peaks in Figuer (13) could be seen on the $[Ni_2(H_2L^2)(H_2O)_2Cl_2]$TGA curve. The first peak was discovered between (58.03 - 102.70 ^oC) and it was accompanied with a mass loss calculation of 8.08% that was attributed to the mass loss of (C_6H_{12}) molecules. The second peak, which was discovered between (339.05-411.61^oC), was accompanied by an 7.18% calculated mass loss due to the breakdown of (N, H_2O, 2Cl) molecules. The third peak was found between (428.87 – 535.46 ^oC) with a mass loss of 6.970% calculated that was attributed to the mass loss of (N, H_2O, 2Cl) molecules.(Ali *et al*,2007).

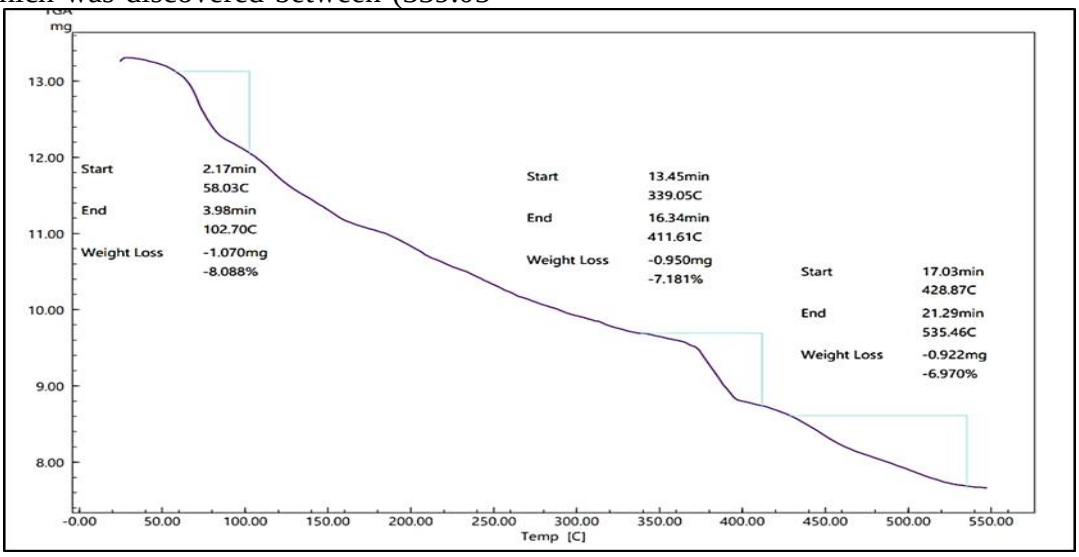

Figure 13. TGA curves of the $[Ni_2(H_2L^2)(H_2O)_4\ Cl_2\ ]$

Molaer conductivity measurement for the complexe: Molar conductivity measurement for the complexes A compound's conductance can be calculated using its measurement of conductivity nonelectrolyte with concentrate (1*10-3) nature of the of the (H_2L^1) and (H_2L^2) complexes . The molar nonelectro-conductivity of complexes listed in Table (5)and (6) in (DMSO) solvent

Table 5.The molar conductivity of the (H_2L^1)complexes

Compound	No Compound m S.cm2 molarc-1 Ratio
$[Mn_2(H_2L^1)(H_2O)_4\ Cl_2\ ]$	19.5
$[Co_2(H_2L^1)(H_2O)_4\ Cl_2]$	16.7
$[Ni_2(H_2L^1)(H_2O)_4Cl_2]$	23.2
$[Cu_2(H_2L^1)Cl_2]$	18.9
$[Cd_2(H_2L^1)Cl_2]$	17.8

Table 6. The molar conductivity of the (H_2L^2) complexes

Compound	No Compound m S.cm2 molar–1 Ratio
$[Mn_2(H_2L^2)(H_2O)_4\ Cl2\ ]$	20.4
$[Co_2(H_2L^2)(H_2O)_4\ Cl2]$	21.2
$[Ni_2(H_2L^2)(H_2O)_4Cl2]$	21.6
$[Cu_2(H_2L^2)Cl2]$	20.7
$[Cd_2(H_2L^2)Cl2]$	19.3

Biological activity complexes and ligands: In addition to the one species of fungi studied (*Candida*), microbiological activity against Gram-positive bacteria (*Staphylococcus aurous and Bacillus subtitles*) and Gram-negative bacteria (*Klebseilla pneumonia and Pseudomonas aeruginosa*) (Zaid &Alrubeii, 2023) for the ligands and their metal complexes were tested in Table(7). Alone solution of DMSO studied and showed no activity against organisms. The test organisms inoculated with agar media, and (100 µg/ml) a solution of the tested compound was separately, placed in a 6 mm diameter plates in the agar medium. The inhibition zones were measured after 24 hours' incubation,. The bacteria and fungi were chosen because of their well-known effects on a range of diseases; they also show different levels of resistance to drugs and drug compounds. The zone of inhibition for the ligand and its complexes was effective.(Khadij &Hassan, 2022)

Iraqi Journal of Agricultural Sciences –2026:57(2):663-675
P-ISSN: 0075- 0530 /E-ISSN: 2410-0862
DOI: https://doi.org/10.36103/x6kpsf31

Table 7.inhibition zone ligands and complexes against pathogenic bacteria and fungi
Inhibition zone mm ligands and complexes

Complexes	*Klebseilla pneumonie*	*Pseudomoas aeruginosa*	*Bacillus subtilus*	*Staphylococus aureus*	*Candida albicans*
gentamicin	-	8	-	20	20
H_2L^1	8	8	13	16	18
$[Ni_2(H_2L^1)(H_2O)_4Cl_2]$	12	13	16	15	20
$[Mn_2(H_2L^1)(H_2O)_4Cl_2]$	13	12	15	16	16
$[Cu_2(H_2L^1)Cl_2]$	13	1	15	17	20
H_2L^2	9	9	14	15	16
$[Cu_2(H_2L^2)Cl_2]$	13	11	16	15	16
$[Ni_2(H_2L^2)(H_2O)_4Cl_2]$	13	10	18	16	18
$[Co_2(H_2L^2)(H_2O)_4Cl_2]$	14	12	16	15	18

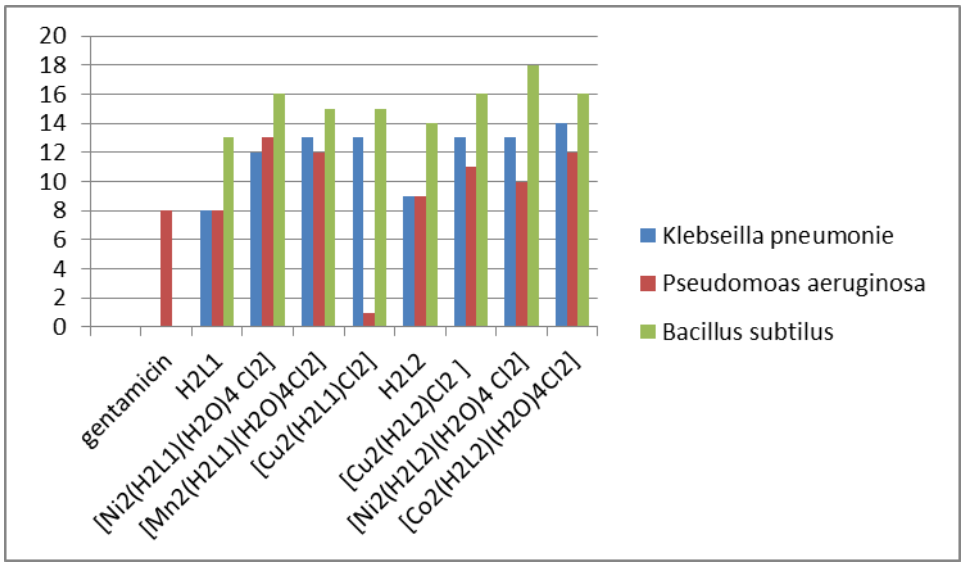

Figure 14. The inhibition zones diameter (mm) against (*K. pneumonie* , *P. aeruginosa, S. aureus, B. Subtilis, and Candida*

CONFLICT OF INTEREST

The authors declare that they have no conflicts of interest.

DECLARATION OF FUND

The authors declare that they have not received a fund.

REFERENCES

Aemed, I. A, and Y. I. Enaam .2022. New metal complexes with AZO ligand; synthesis, Spectral characterisation and biological evaluation, Original Article,m16,(07):551-553 https://doi.org/10.53350/pjmhs22167550

Ali, M. A, A. H.Ahmed , T. A.M, and B. H .Mohamed.2007. Chelates and corrosion inhibition of newly synthesized schiff bases derived from o-tolidine, Transition Metal Chemistry 32:461–467

Baidaa, K .A , M. J. Al-Jeboori and H. Potgieter .2021. Metal complexes of multidentate N2S2 heterocyclic schiff-base ligands; Formation, structural characterisation and biological activity publishing , J. Phys.:12-36 Conf. Ser. 1879 022074 http://dx.doi.org/10.13140/RG.2.2.30677.55526

Bashandy, M. S, F.A.Mohammed , M.M.El-Molla , M. B. Sheier and A. H. Bedair.2016. Synthesis of novel acid dyes with coumarin moiety and their utilization for dyeing wool and silk fabrics. open Journal of Medicinal Chemistry 6(01), 18- 35 DOI: 10.4236/ojmc.2016.61002

Dhekra, J. H, and S.M. Mahdi.2023. Preparation, characterization, and biological

study of new hlogenated azo-schiff base ligands and their complexes; Journal of Medicinal and Chemical Sciences 6 (7) 1555-1576 https://doi.org/10.26655/JMCHEMSCI.2023.7.8

El-Sonbati, A.Z, M.A Diab, A.A El-Bindary, A.F. Shoair and N.M. Beshry.2016. Thermal properties, geometrical structures, antimicrobial activity and DNA binding of supramolecular azo dye complexes. Journal of Molecular Liquids, 218,400- 420. https://doi.org/10.1016/j.molliq.2016.02.043

Eman,M,A. W. M,Alwan, and H. H,Alkam.2020. New mixed ligand complexes of new schiff base 4,4'- ((naphthalen-1-ylimino) methylene) dibenzene-1,3-diol and 8-hydroxy quinoline: synthesis, spectral characterization, Thermal studies and Biological Activities ;11(8):725-735 https://www.researchgate.net/publication/348974826

Enaam, I. Y, A. K. Hussien and H. A. Hassan.2020, CoII, NiII and CdII complexes derived from mixed azo-ligand schiff-base ligands: formation, characterisation, thermalanalysis and biological study, Plant Archives , 20 (1). 2405-2411, n at: https://www.researchgate.net/publication/347356120

Haider, M. H and F. F. Karam.2022. Synthesis, identification, biological activity and anti-cancer activity studies of hetrocyclic ligand azo-schiff base with Au(III) complex, Egypt. J. Chem. 65, (1): 327-334 . https://doi.org/10.21608/ejchem.2021.80392.3980

Hasan, A. H ;Fluorescence.2017. Biological activity and spectroscopic studies of azo-linked schiff base ligand type (ONO) and its complexes with CrIII, CoII NiII and CdII ions Ibn Al-Haitham Jour. for Pure & Appl. Sci. 30 (3) 30(3):114. http://dx.doi.org/10.30526/30.3.1607

Hasan. A. H, B.M. Sarhan, and W. M. Alwan .2013. Synthesis,characterization and biological activity of azo-linked schiff base ligand type (ONO) and its complexes with CrIII, MnII and FeII ions Al-Mustansiriyah J. Sci. 24,(6), :50-55

Khadija F. M and H .A. Hassan. 2022. Synthesis, chemical and biological activity studies of azo-schiff base ligand and its metal complexes, Chemical. Chem. Methodol. 6(12) 905-913, DOI:10.22034/CHEMM.2022.353591.1584

Kheirkhahi, M , B.Shaabani and H.S. Kafil.2021. Calix [4] arene-based thiosemicarbazide schiff-base ligand and its transition metal complexes: synthesis and biological assessment. Journal of the Iranian Chemical Society. 18 (12), 3429-3441 https://doi.org/10.1007/s13738-021-02281-1

Mohammad, J. A, H.H. Altawel, and R. M. Ahamd .2010. New metal complexes of N2S2 tetradentate ligands: synthesis and spectral studies, Inorganica Chimica Acta 363(6) 1301–1305 doi:10.1016/j.ica..11.040

Muna, A .H, and I. K. Kareem.2020. Synthesis and characterization of some transition metal complexes with new azo- schiff base ligand 3,4-bis(((1E,2E)-2-((2-((4-((Z)- (3-Hydroxyphenyl)Diazenyl)Naphthalen-1-yl)amino) ethyl)imino)- 1,2-Diphenylethylidene) Amino)Phenyl)(phenyl) Methanone, Egypt.J.Chem. 63(1) 301 - 313 doi:10.21608/ejchem.2019.18924.2166

Naureen.B, G.A.Miana, K.Shahid, M.Asghar, S.Tanveer, and A.Sarwar.2021. Iron(III) and zinc(II) monodentate Schiff base metal complexes: Synthesis, characterisation and biological activities, Malaysian Journal of Chemistry, 23(3) 55-73 https://doi.org/10.1016/j.molstruc.2021.129946

Rehab,A and M.Al-Hassani.2016. Synthesis, characterization, antimicrobial and theoretical studies of V(IV), Fe(III), Co(II), Ni(II), Cu(II), and Zn(II) complexes with bidentate (NN) donar azo dye ligand, Baghdad Science Journal, .13(4), :794-800 https://doi.org/10.21123/bsj.2016.13.4.0793

Reham,H.H, and H.A.Hassan .2022. Synergism antibacterial activity for novel synthesized schiff base ligands and semithiosemicarbazones with ß-diketones and 4-aminoantipyrine. Article / inveSstgacion ;7(3) 43 http:// doi. 10.21931/RB/2022.07.03.43

Iraqi Journal of Agricultural Sciences –2026:57(2):663-675
P-ISSN: 0075- 0530 /E-ISSN: 2410-0862
DOI: https://doi.org/10.36103/x6kpsf31

Said.B, S.ELharfi and A. El Harfi.2017. Classifications, properties and applications of textile dyes, J. Envir. Eng. 3 (3). 311-320

Said, B, S.Mrabet , and A. Elharfi .2020. Classifications, properties, recent synthesis and applications of azo dyes, Heliyon 6 e03271. https://doi.org/10.1016/j.heliyon.2020.e03271

Shaima, M. R and A. A. Salih.2022. Mn(II),Fe(III),Co(II) and Rh(III) complexes with azo ligand:synthesis, characterization, thermal analysis and bioactivity, Baghdad Science Journal : 20(3): 642-660. **:** https://doi.org/10.21123/bsj.2022.7289

Wasan, M. A, R .M. Ahmed, E. I. Yousif, B.K. Al-Rubaye, K.M. Sultan and H. A. Hasan.2019.New mixed ligand of dithiocarbamate and 8, hydroxyqunoline with some complexes of schiff base ligands : synthises, spectral analysis and biologlcal activity, Biochem. Cell. Arch. 19 (2) : 4535-4543 DOI : 10.35124/bca.2019.19.2.4535.

Zaid, I.H and A. M.S. Alrubeii.2023. Effect of replacement nitriteby beet root and silybum marianum powder inphysicalcharacteristics and lipid oxidation for paster, Iraqi Journal of Agricultural Sciences :54(4):1131-1136,https://doi.org/10.36103/ijas.v54i4.1806.

Iraqi Journal of Agricultural Sciences –2026:57(2):663-675
P-ISSN: 0075- 0530 /E-ISSN: 2410-0862
DOI: https://doi.org/10.36103/x6kpsf31

المعقدات الفلزية لليكندات الكركمين وثنائي بنزيل ميثان ، الشكل الهندسي،ودراسة الفعالية البايولوجية

فاطمة رشيد علي حسن احمد حسن

قسم الكيمياء،كلية التربية للعلوم الصرفة (أبن الهيثم)،جامعة بغداد،بغداد، العراق

المستخلص

هدفت هذه الدراسة إلى بحث تخليق وتوصيف نوعين من الروابط (azo-linked Schiff-base) مع مركباتها. تم الحصول على المركب الأولي (W) من خلال تفاعل 1-Naphthyl amine مع O-tolidin في الماء كمذيب بنسبة مولية 2:1. يتم تصنيع روابط Azo-linked Schiff-base عن طريق تفاعل 3،3 3, 3-(E))bis-5,5'-dimethyl-3,3' -pyridin-3-yldiazenyl)-[1,1'-biphenyl]-4,4'-diamine with curcumun or dibenziyl methan for obtaining 4, 4', 4", 4"'- ((1E, 1'E, 6E, 6'E) - ((3, 3'- dimethyl-5, 5'-bis((E)-pyridin-3-yldiazenyl)-[1,1'-biphenyl]-4,4'-diyl) bis (azaneylylidene)) bis(5-hydroxyhepta-1,6-diene-1,7-diyl-3-ylidene)) tetrakis (2-methoxyphenol) (H2L1) or 3,3'-((3,3'-dimethyl-5,5'-bis((E)-naphthalen-1- yldiazenyl)- [1,1'-biphenyl]- 4,4'-diyl) bis (azaneylylidene)) bis (1,3-diphenylpropan-1-ol) (H2L2). تم تحضير هذه المركبات المعقدة عن طريق تفاعل أملاح أيونات المعادن CoII وMnII وCuII وNiII وCdII مع روابط azo-linked Schiff-base المرتبطة برابطة azo-linked بنسبة مولية (2:1). شملت تقنيات التحليل الطيفي والتحليلي توصيف الروابط والمركبات المحضرة، بما في ذلك قياسات التوصيلية، والتحليل الدقيق، والتحليل الحراري، والحساسية المغناطيسية (للمركبات المعقدة)، بالإضافة إلى مطيافية الرنين النووي المغناطيسي، ومطيافية NMR, UV-Vis و التحليل الطيفي FTIR.

الكلمات المفتاحية : قواعد كشف ,ازو,نفثايل امين, تولودين,كركمين, داي بنزا امين

*جزء من اطروحة دكتوراه للباحث الأول